

Cessna T-37, Image Source - Drawing Database

Flight Dynamics Project 2023 - 2024

Stability Analysis of the Cessna T-37

Kanak Agarwal

Roll Number - 31

Registration Number - 210933058

Batch of 2021-2025

Manipal Institute of Technology

Bachelor of Technology in Aeronautical Engineering

October 10, 2023

Contents

1	Introduction	1
2	Flight Conditions	1
3	Modelling the Wing Lift Slope Coefficient	1
4	Modelling the Effect of Downwash	2
5	Aerodynamic Center of the Wing	2
6	Effect of the Fuselage on the Aerodynamic Center	2
7	Modelling the Horizontal Tail Lift Slope Coefficient	3
8	Aircraft Aerodynamic Center	4
9	Static Margin	4
10	Contribution to the Dihedral Effect	4
11	Modelling Stability Derivatives	5
11.1	C_{L_α}	5
11.2	C_{m_α}	5
11.3	C_{L_q}	5
11.4	C_{m_q}	5
11.5	C_{Y_β}	6
11.6	C_{n_β}	6
11.7	C_{L_p}	6
11.8	C_{L_β}	7
11.9	C_{n_r}	7
11.10	C_{m_u}	7
11.11	$C_{T_{X_u}}$	8
11.12	C_{D_u}	8
12	Static Stability Criteria	8
13	Conclusion	8
14	References	9
15	Appendix	9
15.1	Geometric Parameters of the Aircraft (Cessna T-37)	9
15.2	MATLAB Code	10

1 Introduction

The following report outlines the methodology and the results of the stability analysis conducted on the Cessna T-37 as a part of the Flight Dynamics coursework for the academic year 2023-2024 at the Manipal Institute of Technology, Karnataka, India.

The stability analysis was conducted using MATLAB. L^AT_EX was used to formulate the report. Once the results were obtained, they were analysed, and suitable conclusions were drawn from the respective values.

The aircraft's initial geometric parameters were taken from Appendix C of reference [1]. These values are outlined in the Appendix of this report. These values were built upon to conduct these analyses.

2 Flight Conditions

The flight conditions chosen to analyse the static stability of the aircraft are as follows:

Parameter [unit]	Value	Parameter [unit]	Value
Altitude [ft]	30,000	Mach Number	0.459
V_{P_1} [ft/s]	456	q_1 [lbs/ft ²]	92.7
α_1 [deg]	2°	S [ft ²]	182
\bar{c} [ft]	5.1	b [ft]	33.8
X_{CG} [ft]	0.27	W [lbs]	6,360

3 Modelling the Wing Lift Slope Coefficient

The empirical relations in reference [1] can be applied for subsonic operation, moderate sweep angles and reasonably moderate aspect ratios. This particular aircraft satisfies these conditions, and the following relations were used,

$$C_{L_\alpha} = \frac{2\pi AR}{2 + \sqrt{\left(\left[\frac{AR^2(1-M^2)}{k^2}\right]\left(1 + \frac{\tan^2(\Delta_{0.5})}{1-M^2}\right)\right) + 4}}$$

where k for AR ≥ 4 is given by,

$$k = 1 + \frac{[(8.2 - 2.3\Lambda_{LE}) - AR(0.22 - 0.153\Lambda_{LE})]}{100}$$

On calculation, this turns out to be,

$$C_{L_\alpha} = 5.5746$$

The empirical relations outlined above are called the Polhamus formulae and have been modelled from correlation studies conducted over extensive wind tunnel data.

4 Modelling the Effect of Downwash

An important longitudinal aerodynamic effect is the downwash effect. In general, this effect can be considered an aerodynamic "interference" generated by the wing on the horizontal tail due to the system of vortices created by the wing.

The following relationship is used to model the downwash effect,

$$\left(\frac{d\epsilon}{d\alpha} \right) = f(M, m, r, \Lambda_{LE}, \lambda, AR)$$

The closed form expression is given by,

$$\left(\frac{d\epsilon}{d\alpha} \right) \Big|_M = \left(\frac{d\epsilon}{d\alpha} \right) \Big|_{M=0} \sqrt{1 - M^2}$$

where,

$$\left(\frac{d\epsilon}{d\alpha} \right) \Big|_{M=0} = 4.44 \left(K_{AR} K_\lambda K_{mr} \sqrt{\cos(\Lambda_{0.25})} \right)$$

with,

$$K_{AR} = \frac{1}{AR} - \frac{1}{1 + AR^{1.7}}, \quad K_\lambda = \frac{10 - 3\lambda}{7}, \quad K_{mr} = \frac{1 - m/2}{r^{0.333}}$$

The sweep angle at any point on the wing can be found using,

$$\tan(\Lambda_x) = \tan(\Lambda_{LE}) - \frac{4x(1 - \lambda)}{AR(1 + \lambda)}$$

The downwash effect is calculated to be,

$$\left(\frac{d\epsilon}{d\alpha} \right) \Big|_M = 0.3758$$

5 Aerodynamic Center of the Wing

The Aerodynamic Center of the wing can be found using the relation,

$$\bar{x}_{AC_W} = K_1 \left(\frac{x'_{AC}}{c_R} - K_2 \right)$$

where K_1 and K_2 are geometric parameters of the wing and can be determined from the empirical plots. This turned out to be,

$$\bar{x}_{AC_W} = 0.1150$$

6 Effect of the Fuselage on the Aerodynamic Center

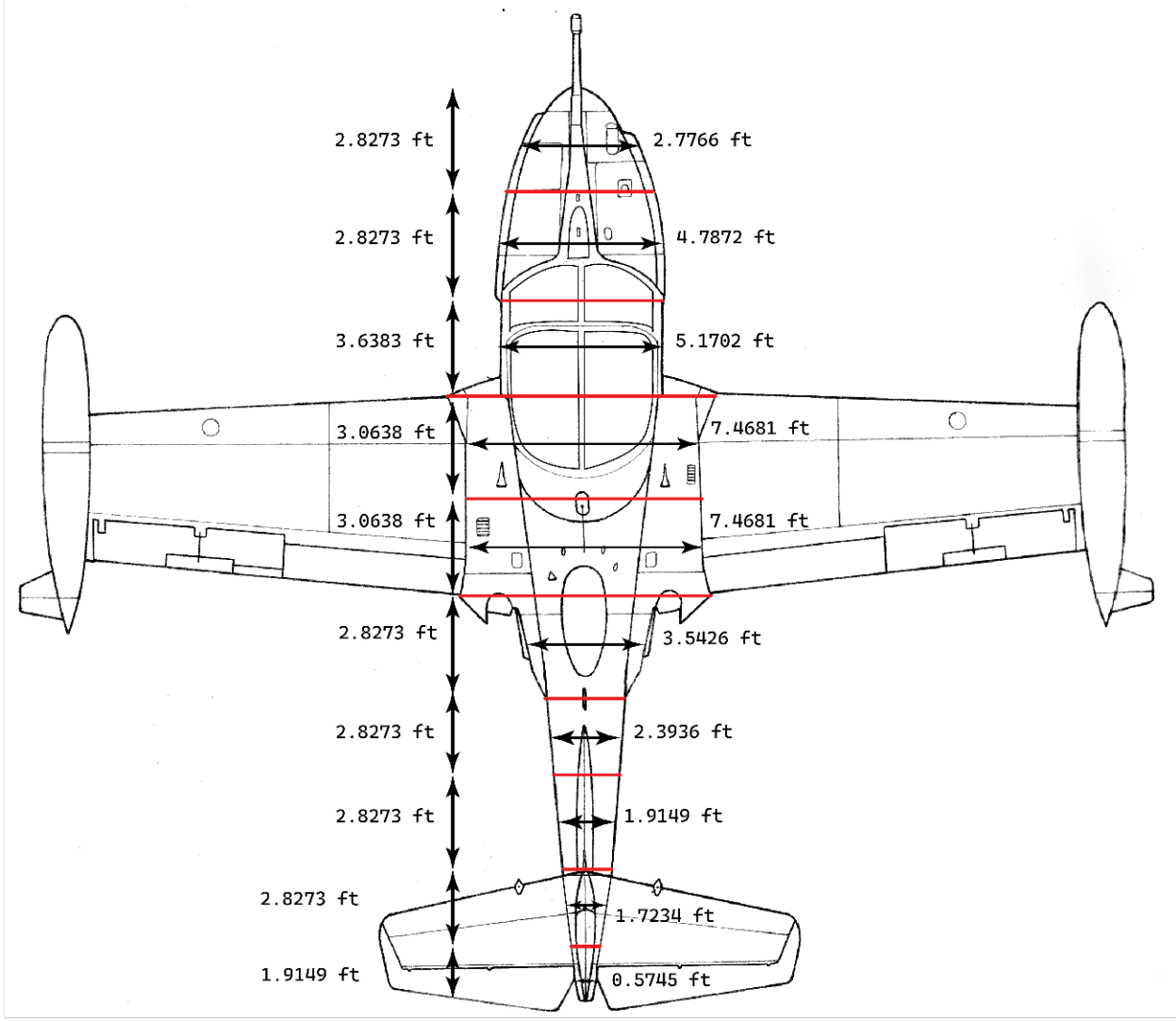
The shift in the aerodynamic center due to the addition of the fuselage is given by,

$$\Delta \bar{x}_{AC_B} = \frac{\left(\frac{\bar{q}}{36.5} \frac{C_{L_{\alpha W}}}{0.08} \right)}{\bar{q} S \bar{c} C_{L_{\alpha W}}} \sum_{i=1}^N w_{B_i}^2 \left(\frac{d\epsilon}{d\alpha} \right)_i \Delta x_i$$

where,

$$\left(\frac{d\epsilon}{d\alpha}\right)_i = \left(\frac{x_i}{x_H}\right) \left(1 - \left.\frac{d\epsilon}{d\alpha}\right|_{m=0}\right)$$

w_{B_i} and x_i are geometric parameters for the discretised aircraft sections in accordance with Munk's theory. These parameters are shown below,



The final shift of the aerodynamic center due to the body is,

$$\Delta \bar{x}_{AC_B} = -0.0011$$

7 Modelling the Horizontal Tail Lift Slope Coefficient

The empirical relations in reference [1] can be applied for subsonic operation, moderate sweep angles and reasonably moderate aspect ratios. This particular aircraft satisfies these conditions, and the following relations were used,

$$C_{L_{\alpha_H}} = \frac{2\pi AR_H}{2 + \sqrt{\left(\left[\frac{AR_H^2(1-M^2)}{k^2}\left(1 + \frac{\tan^2(\Delta_{0.5H})}{1-M^2}\right)\right] + 4\right)}}$$

where k for $AR_H \geq 4$ is given by,

$$k = 1 + \frac{[(8.2 - 2.3\Lambda_{LE_H}) - AR_H(0.22 - 0.153\Lambda_{LE_H})]}{100}$$

On calculation, this turns out to be,

$$C_{L_{\alpha_H}} = 4.3335$$

The empirical relations outlined above are called the Polhamus formulae and have been modelled from correlation studies conducted over extensive wind tunnel data. The results conforms to the trend of the $C_{L_{\alpha_H}}$ being lower of the C_{L_α} value.

8 Aircraft Aerodynamic Center

The aircraft's aerodynamic center can be estimated using the relation,

$$\bar{x}_{AC} = \frac{\bar{x}_{AC_{WB}} + \frac{C_{L_{\alpha_H}}}{C_{L_{\alpha_H}}} \eta_H \frac{S_H}{S} (1 - \frac{d\epsilon}{d\alpha}) \bar{x}_{AC_H}}{1 + \frac{C_{L_{\alpha_H}}}{C_{L_{\alpha_H}}} \eta_H \frac{S_H}{S} (1 - \frac{d\epsilon}{d\alpha})} = 0.4486$$

9 Static Margin

The static margin is given by,

$$SM = \bar{x}_{CG} - \bar{x}_{AC} = -0.0327$$

Since it is a negative value, the CG is ahead of the AC, and hence the aircraft is stable.

10 Contribution to the Dihedral Effect

The individual contributions to the dihedral effect are evaluated separately and combined into one integrated term. The contributions to the dihedral effect are as follows,

- * Wing contribution due to the geometric dihedral angle
- * Wing contribution due to the wing-fuselage positions
- * Wing contribution due to the sweep angle
- * Wing contribution due to the aspect ratio
- * Wing contribution due to the twist angle
- * Body (fuselage) contribution

$C_{L_{\beta_{WB}}}$ is given by,

$$\begin{aligned} C_{L_{\beta_{WB}}} &= 57.3 \cdot C_{L_1} \left[\left(\frac{C_{L_\beta}}{C_{L_1}} \right)_{\Lambda_{c/2}} K_{M_\Lambda} K_f + \left(\frac{C_{L_\beta}}{C_{L_1}} \right)_{AR} \right] + \\ &57.3 \left\{ \Gamma_W \left[\frac{C_{L_\beta}}{\Gamma_W} K_{M_\Gamma} + \frac{\Delta C_{L_\beta}}{\Gamma_W} \right] + (\Delta C_{L_\beta})_{Z_W} + \epsilon_W \tan \Lambda_{c/4} \left(\frac{\Delta C_{L_\beta}}{\epsilon_W \tan \Lambda_{c/4}} \right) \right\} \\ &= -0.0615 \end{aligned}$$

11 Modelling Stability Derivatives

11.1 C_{L_α}

Assuming a η_H of 0.9, the derivative is obtained using the relation,

$$C_{L_\alpha} = C_{L_{\alpha_W}} + C_{L_{\alpha_H}} \eta_H \frac{S_H}{S} \left(1 - \frac{d\epsilon}{d\alpha} \right) = 5.5746$$

11.2 C_{m_α}

This derivative is calculated using,

$$C_{m_\alpha} = C_{L_{\alpha_W}} (\bar{x}_{CG} - \bar{x}_{AC_{wb}}) + C_{L_{\alpha_H}} \eta_H \frac{S_H}{S} \left(1 - \frac{d\epsilon}{d\alpha} \right) (\bar{x}_{AC_H} - \bar{x}_{AC_{WB}}) = -1.1815$$

11.3 C_{L_q}

The modelling of this derivative is given by,

$$C_{L_q} = C_{L_{q_W}} + C_{L_{q_H}}$$

where $C_{L_{q_H}}$ is,

$$C_{L_{q_H}} = 2C_{L_{\alpha_H}} \eta_H \frac{S_H}{S} (\bar{x}_{AC_H} - \bar{x}_{CG})$$

and $C_{L_{q_W}}$ is given by,

$$C_{L_{q_W}} = \left[\frac{AR + 2\cos\Lambda_{c/4}}{AR \cdot B + 2\cos\Lambda_{c/4}} \right] \cdot C_{L_{q_W}}|_{M=0}$$

where B is,

$$B = \sqrt{1 - M^2(\cos\Lambda_{c/4})^2}$$

Finally the value of C_{L_q} is calculated to be,

$$C_{L_q} = 8.7064$$

11.4 C_{m_q}

This derivative is evaluated using the relation,

$$C_{m_q} = C_{m_{q_H}} + C_{m_{q_W}}$$

where,

$$C_{m_{q_H}} = -2C_{L_{\alpha_H}} \eta_H \frac{S_H}{S} (\bar{x}_{AC_H} - \bar{x}_{CG})^2$$

and,

$$C_{m_{q_W}} = \left[\begin{array}{l} \frac{AR^3 \tan^2 \Lambda_{c/4}}{AR \cdot B + 6\cos\Lambda_{c/4}} + \frac{3}{B} \\ \frac{AR^3 \tan^2 \Lambda_{c/4}}{AR + 6\cos\Lambda_{c/4}} + 3 \end{array} \right] \cdot C_{m_{q_W}}|_{M=0}$$

where,

$$C_{m_{q_W}}|_{M=0} = -K_q C \cos\Lambda_{c/4} C_{L_{\alpha_W}}|_{M=0}$$

$$B = \sqrt{1 - M^2(\cos\Lambda_{c/4})^2}$$

$$C = \left\{ \frac{AR(0.5|(\bar{x}_{AC_W} - \bar{x}_{CG})| + 2|(\bar{x}_{AC_H} - \bar{x}_{CG})|^2)}{AR + 2\cos\Lambda_{c/4}} + \frac{1}{24} \left(\frac{AR^3\tan\Lambda_{c/4}}{AR + 6\cos\Lambda_{c/4}} \right) + \frac{1}{8} \right\}$$

Therefore,

$$C_{m_q} = -20.4800$$

11.5 C_{Y_β}

The modelling of this derivative is given by,

$$C_{Y_\beta} = C_{Y_{\beta_W}} + C_{Y_{\beta_B}} + C_{Y_{\beta_H}} + C_{Y_{\beta_V}}$$

$C_{Y_{\beta_H}} = 0$, since the dihedral angle of the horizontal tail is 0. Further,

$$C_{Y_{\beta_W}} = -0.0001|\Gamma_W| \cdot 57.3$$

$$C_{Y_{\beta_B}} = -2 \cdot K_{int} \cdot \frac{S_{P \rightarrow V}}{S}$$

$$C_{Y_{\beta_V}} = -K_{Y_V} \cdot |C_{L_{\alpha_V}}| \eta_V \cdot \left(1 + \frac{d\sigma}{d\beta}\right) \frac{S_V}{S}$$

Therefore,

$$C_{Y_\beta} = -0.5151$$

11.6 C_{n_β}

This derivative is calculated using the relation,

$$C_{n_\beta} = C_{n_{\beta_W}} + C_{n_{\beta_B}} + C_{n_{\beta_H}} + C_{n_{\beta_V}}$$

At small angles of attack, $C_{n_{\beta_W}} = 0$. Also, due to the zero dihedral angle of the horizontal tail, $C_{n_{\beta_H}} = 0$. Further,

$$C_{n_{\beta_B}} = -57.3 \cdot K_N K_{Rt} \frac{S_{B_s}}{S} \frac{l_B}{b}$$

$$C_{n_{\beta_V}} = -C_{Y_{\beta_V}} \cdot \frac{X_V \cos\alpha_1 + Z_V \sin\alpha_1}{b}$$

Therefore,

$$C_{n_\beta} = 0.5658$$

11.7 C_{L_p}

The derivative is modelled using the following relation,

$$C_{l_p} = C_{l_{p_{WB}}} + C_{l_{p_H}} + C_{l_{p_V}}$$

where,

$$C_{l_{p_{WB}}} = C_{l_{p_W}} = RDP \cdot \frac{k}{\beta}$$

$$C_{l_{p_H}} = \frac{1}{2} (C_{L_{p_W}}) \Big|_H \frac{S_H}{S} \left(\frac{b_H}{b} \right)^2$$

and,

$$(C_{l_{p_W}}) \Big|_H = RDP_H \cdot \frac{k_H}{\beta_H}$$

where,

$$k_H = \frac{(C_{L_{\alpha_H}})_W \Big|_M \cdot \beta_H}{2\pi}$$

Further,

$$C_{l_{p_V}} = 2C_{Y_{\beta_V}} \left(\frac{z_V}{b} \right)^2$$

Therefore,

$$C_{n_\beta} = -0.5432$$

11.8 C_{L_β}

This derivative is evaluated using,

$$C_{L_\beta} = C_{L_{\beta_{WB}}} + C_{L_{\beta_H}} + C_{L_{\beta_V}}$$

$C_{L_{\beta_H}} = 0$, since the dihedral angle of the horizontal tail is 0. Further,

$$C_{L_{\beta_V}} = -K_{Y_V} \cdot |C_{L_{\alpha_V}}| \eta_V \cdot \left(1 + \frac{d\sigma}{d\beta} \right) \frac{S_H}{S} \cdot \frac{Z_V \cos \alpha_1 - X_V \sin \alpha_1}{b}$$

Therefore,

$$C_{L_\beta} = -0.0996$$

11.9 C_{n_r}

This derivative is modelled using the relation,

$$C_{n_r} = C_{n_{r_w}} + C_{n_{r_V}}$$

where,

$$C_{n_{r_W}} = \left(\frac{C_{n_r}}{C_{L_1}} \right) \cdot C_{L_1}^2$$

and,

$$C_{n_{r_V}} = 2C_{Y_{\beta_V}} \cdot \frac{(X_V \cos \alpha_1 + Z_V \sin \alpha_1)^2}{b^2}$$

Therefore,

$$C_{n_r} = -0.1118$$

11.10 C_{m_u}

This parameter is negligible at the subsonic conditions associated with the operating Mach number of this aircraft. In general, this parameter plays a significant role only during transonic operation. Therefore,

$$C_{m_u} = 0$$

11.11 $C_{T_{X_u}}$

It is the coefficient modelling the thrust variation along X_S associated with small variations in the linear speed in the forward direction. The quantification of this effect depends on the specific propulsion system used onboard the aircraft. Further,

$$C_{T_{X_u}} = -0.07$$

11.12 C_{D_u}

For this particular aircraft, it is given that,

$$C_{D_u} = 0$$

12 Static Stability Criteria

Stability Criteria	Value	Conclusion
SC #1: $(C_{T_{X_u}} - C_{D_u}) < 0$	$C_{T_{X_u}} = -0.07, C_{D_u} = 0$	STABLE
SC #2: $C_{Y_\beta} < 0$	$C_{Y_\beta} = -0.5151$	STABLE
SC #3: $C_{L_\alpha} > 0$	$C_{L_\alpha} = 5.5746$	STABLE
SC #4: $C_{m_\alpha} < 0$	$C_{m_\alpha} = -1.1815$	STABLE
SC #5: $C_{n_\beta} > 0$	$C_{n_\beta} = 0.5658$	STABLE
SC #6: $C_{l_p} < 0$	$C_{l_p} = -0.5432$	STABLE
SC #7: $C_{m_q} < 0$	$C_{m_q} = -20.4800$	STABLE
SC #8: $C_{n_r} < 0$	$C_{n_r} = -0.1118$	STABLE
SC #9: $C_{L_\beta} < 0$	$C_{L_\beta} = -0.0996$	STABLE
SC #10: $C_{m_u} > 0$	$C_{m_u} = 0$	MARGINALLY STABLE

13 Conclusion

The aircraft in this particular flight condition meets all the static stability criteria. Hence, it can be concluded that the aircraft is statically stable for this specific flight condition.

14 References

[1] Marcello R. Napolitano, "Aircraft Dynamics From Modelling to Simulation", Wiley - 2012

15 Appendix

15.1 Geometric Parameters of the Aircraft (Cessna T-37)

Geometric Parameters [unit]	Value	Geometric Parameters [unit]	Value
A [ft]	12.4	X_{HV} [ft]	1.5
b [ft]	33.8	X_{WHR} [ft]	15.9
b_H [ft]	14.0	X_1 [ft]	26.6
b_V [ft]	14.0	y_{A_1} [ft]	9.9
\bar{c} [ft]	5.47	y_{A_0} [ft]	16.6
$\bar{c}_{Aileron}$ [ft]	1.2	y_{R_I} [ft]	0
\bar{c}_R [ft]	1.4	y_{R_F} [ft]	4.4
$\bar{c}_{wing \ (At \ aileron)}$ [ft]	4.9	y_V [ft]	1.7
c_r [ft]	6.2	Z_H [ft]	-3.1
c_{r_H} [ft]	4.6	Z_{RS} [ft]	3.6
c_{r_V} [ft]	6	z_1 [ft]	4.3
c_T [ft]	4.5	z_2 [ft]	2.1
c_{T_H} [ft]	2.2	Z_{HS} [ft]	-3.1
c_{T_V} [ft]	2.5	z_{max} [ft]	4.4
d [ft]	4	Z_W [ft]	0
l_b [ft]	29.2	Z_{WHR} [ft]	3
l_{cg} [ft]	11.4	Γ_H [deg]	0
r_1 [ft]	2.2	Γ_W [deg]	3
S [ft ²]	182	ϵ_H [deg]	0
S_{BS} [ft ²]	80.2	ϵ_W [deg]	0
$S_{f\ avg}$ [ft ²]	8.7	Δ_{LE} [deg]	1.5
$S_{P\rightarrow V}$ [ft ²]	1.9	Δ_{LE_H} [deg]	12.5
w_{max} [ft]	9	Δ_{LE_V} [deg]	33
X_{AC_R} [ft]	5.1		

15.2 MATLAB Code

```

1 %% Aircraft DATA Cessna T37 A
2 AR = 6.27; % Aspect Ratio
3 A = 12.4; % ft - Distance between Nose and AC of C_tip
4 b = 14; % ft - wingspan
5 b_H = 14; % ft - Horizontal Tail span
6 b_V = 4.8; % ft - Vertical Tail span
7 mac_w = 5.47; % ft - MAC wing
8 c_ail = 1.2; % ft - Aileron chord
9 c_R = 1.4; % ft - Rudder Chord
10 C_r = 6.2; % ft - Root Chord Wing
11 C_r_H = 4.6; % ft - Root Chord Horizontal Tail
12 C_r_V = 4.6; % ft - Root Chord Vertical Tail
13 C_t = 4.5; % ft - Tip Chord Wing
14 C_t_H = 2.2; % ft - Tip Chord Horizontal Tail
15 C_t_V = 2.5; % ft - Tip Chord Vertical Tail
16 d = 4; % ft - Maximum Fuselage height at Wing Body intersection
17 l_b = 29.2; % ft - Horizontal length of the aircraft
18 l_cg = 11.4; % ft - Moment arm of CG
19 r1 = 2.2; % ft - Fuselage Height (including fin) at Root Chord AC of Vertical tail
20 S_w = 182; % sq. ft - Planform Area of the Wing
21 S_B_s = 80.2; % sq. ft - Fuselage Side Surface Area
22 S_f_avg = 8.7; % sq. ft - Average Fuselage Cross Sectional Area
23 S_p_v = 1.9; % sq. ft - Fuselage Cross-sectional Area where flow turns from Potential to Viscous
24 w_max = 9; % ft - Max Fuselage width (due to engine intakes)
25 X_AC_R = 5.1; % ft - Distance between LE of C_r_V and AC of Rudder
26 X_HV = 1.5; % ft - Distance between LE of C_r_V and LE of C_r_H
27 X_WH_r = 15.9; % ft - Distance between LE of C_r and LE of C_r_H
28 X_WV_r = X_WH_r-X_HV; % ft - Distance between LE of C_r and LE of C_r_V
29 X_1 = 26.6; % ft - Location on the Fuselage where flow turns from Potential to Viscous
30 y_A_1 = 9.9; % ft - Inboard Location of aileron on the wing
31 y_A_0 = 16.6; % ft - Outboard Location of aileron on the wing
32 y_R_I = 0; % ft - Inboard Location of Rudder
33 y_R_F = 4.4; % ft - Outboard Location of Rudder
34 y_V = 1.7; % ft - Vertical distance between FRL and C_r_V
35 Z_H = -3.1; % ft - Vertical distance between FRL and C_r_H
36 Z_R_s = 3.6; % ft - Moment Arm for Rudder
37 z_1 = 4.3; % ft - Fuselage Diameter before canopy
38 z_2 = 2.1; % ft - Fuselage Diameter just before Tail
39 Z_H_s = -3.1; % ft - Vertical Distance Horizontal Stabiliser
40 z_max = 4.4; % ft - Max Fuselage height including canopy
41 Z_W = 0; % ft - Vertical Distance between Wing Root and FRL
42 Z_WH_r = 3; % ft - Vertical Distance between Wing Root axis and Horizontal Tail root axis
43 gamma_H = 0; % deg - Horizontal Tail Dihedral Angle
44 gamma_W = 3; % deg - Wing Dihedral Angle
45 epsilon_H = 2; % deg - Twist Angle Horizontal Stabiliser
46 epsilon_W = 2; % deg - Wing twist angle (aerodynamic twist) - angle between zero lift lines
47 Lambda_LE = 1.5; % deg - Sweep Angle Wing
48 Lambda_LE_H = 12.5; % deg - Sweep Angle Horizontal Stabiliser
49 Lambda_LE_V = 33; % deg - Sweep Angle Vertical Stabiliser
50 Z_WH = 3.1; % ft - Vertical Distance between FRL and ftAC of Horizontal Tail
51
52 %% Flight Conditions DATA
53 h = 30000; % ft - Altitude
54 [T,a,P,rho] = atmosisa(h*.3048); % Flow Properties at 30,000 ft
55 M = 0.459; % Mach Number
56 Vp1 = 456; % ft/s - Perturbation Velocity
57 q = 92.7; % lbs/sq. ft - Dynamic Pressure
58 X_cg = 0.27; % cg location as a fraction of fuselage length
59 W = 6360; % lbs - Weight
60 alpha = 2; % deg - AoA
61 mu = 3.823*10^-4; % Dynamic Viscosity at 30k ft
62

```

```

63 %% Wing Parameters
64 lambda = C_t/C_r;
65 Lambda_LE = Lambda_LE*pi/180;
66 Lambda_LE_half = atan((tan(Lambda_LE))-((2*(1-lambda))/(AR*(1+lambda)))); % Taper Ratio Wing
67 Lambda_LE_quarter = atan((tan(Lambda_LE))-((1-lambda)/(AR*(1+lambda)))); % rad
68 X_mac_w = ((b*(1+(2*lambda)))/(6*(1+lambda)))*tan(Lambda_LE); % rad - Geometric Relation
69 % ft - Distance between LE of C_r and LE of mac
70
71 %% Horizontal Tail Parameters
72 Lambda_LE_H = Lambda_LE_H*pi/180; % rad
73 lambda_H = C_t_H/C_r_H;
74 % Taper Ratio Horizontal Tail
75 mac_H = (2/3)*C_r_H*((1+lambda_H)+(lambda_H)^2)/(1+lambda_H));
76 % ft - MAC of Horizontal Tail
77 X_mac_H = ((b_H*(1+(2*lambda_H)))/(6*(1+lambda_H)))*tan(Lambda_LE_H);
78 % ft - Distance between LE of C_r_H and LE of mac_H
79 S_H = (b_H/2)*C_r_H*(1+lambda_H);
80 % sq. ft - Planform Area Horizontal Tail
81 AR_H = (b_H^2)/S_H;
82 % Aspect Ratio Horizontal Tail
83 Lambda_LE_half_H = atan((tan(Lambda_LE_H))-((2*(1-lambda_H))/(AR_H*(1+lambda_H)))); % rad - Geometric Relation
84 Lambda_LE_quarter_H = atan((tan(Lambda_LE_H))-(((1-lambda_H))/(AR_H*(1+lambda_H)))); % rad - Geometric Relation
85
86 %% Wing Horizontal Tail Geometric Properties
87 X_WH = X_WH_r - (C_r/4) + (C_r_H/4);
88 % ft - distance between Wing root AC and Horizontal Tail root AC
89 m = Z_WH*2/b; % Geometric Parameter
90 r = X_WH*2/b; % Geometric Parameter
91 X_AC_H = X_WH_r + X_mac_H + (mac_H/4)-X_mac_w;
92 % ft - distance between Wing mac AC and Horizontal Tail mac AC
93
94 %% Wing Lift Slope Coefficient
95 k = 1+((8.2-(2.3*Lambda_LE))-AR*(0.22-(0.153*Lambda_LE)))/100; % From Polhamus Formula
96 C_L_alpha_w = (2*pi*AR)/(2+sqrt(((AR^2*(1-M^2)/k^2)*(1+((tan(Lambda_LE_half))^2)/(1-M^2))))+4)); % From Polhamus Formula Mach = M
97 C_L_alpha_w_o = (2*pi*AR)/(2+sqrt(((AR^2*(1/k^2)*(1+((tan(Lambda_LE_half))^2)/(1))))+4)); % From Polhamus Formula Mach = 0
98
99 %% Downwash on Horizontal Tail
100 K_AR = (1/AR)-(1/(1+(AR^1.7)));
101 % Parameter to calculate d epsilon/d alpha at Mach = 0
102 K_lambda = (10-(3*lambda))/7;
103 % Parameter to calculate d epsilon/d alpha at Mach = 0
104 K_mr = (1 - (m/2))/(r^0.333);
105 % Parameter to calculate d epsilon/d alpha at Mach = 0
106 dEps_dalpha_o = 4.44*((K_AR*K_lambda*K_mr*sqrt(cos(Lambda_LE_quarter)))^1.19)); % d epsilon/d alpha at Mach = 0
107 dEps_dalpha = dEps_dalpha_o*(C_L_alpha_w/C_L_alpha_w_o); % d epsilon/d alpha at Flight Conditions
108 alpha_H = alpha*(1-dEps_dalpha); % rad - Effective AoA at Horizontal Tail
109 K_mr_o = 1/(r^0.333);
110 dEps_dalpha_m_o = 4.44*((K_AR*K_lambda*K_mr_o*sqrt(cos(Lambda_LE_quarter)))^1.19)); % d epsilon/d alpha at Mach = 0, m = 0
111
112 %% Wing Aerodynamic Center
113 p1 = (tan(Lambda_LE))/(sqrt(1-(M^2))); % Parameter to determine K1 and K2 from the plots
114 p2 = AR*tan(Lambda_LE); % Parameter to determine K1 and K2 from the plots
115 k1 = 1.15; % Parameter to determine wing AC (from plots)
116 k2 = 0.1; % Parameter to determine wing AC (from plots)
117 xd_AC_Cr = 0.2; % Parameter to determine wing AC (from plots)
118 x_AC_w = k1*(xd_AC_Cr-k2); % ft - Location of Wing AC

```

```

125
126 % Effect of Body on AC Munk's Theory
127 X_H = X_mac_w + X_AC_H - C_r;
128 % ft - Distance between Wing TE and AC of Horizontal Tail MAC
129 w_i = [0.29 0.5 0.54 0.78 0.78 0.37 0.25 0.20 0.18 0.06];
130 s_f = 9/0.94;
131 w_i = w_i.*s_f;
132 x_i = [0.83 0.53 0.19 0.48 0.16 0.15 0.45 0.75 1.05 1.15];
133 % position of fuselage widths (middle of section)
134 x_i = x_i.*s_f;
135 Del_x_i = [0.3 0.3 0.38 0.32 0.32 0.3 0.3 0.3 0.3 0.2];
136 Del_x_i = Del_x_i.*s_f;
137 x_i_c_f = x_i./C_r;
138 x_i_x_H = x_i./X_H;
139 dEps_dalpha_M_m_o = dEps_dalpha_m_o*(C_L_alpha_w/C_L_alpha_w_o);
140 dEps_dalpha_i = [1.1 1.2 1.6 1.3 (x_i_x_H(5)*(1-dEps_dalpha_M_m_o)) ...
141 (x_i_x_H(6)*(1-dEps_dalpha_M_m_o)) (x_i_x_H(7)*(1-dEps_dalpha_M_m_o)) ...
142 (x_i_x_H(8)*(1-dEps_dalpha_M_m_o)) (x_i_x_H(9)*(1-dEps_dalpha_M_m_o)) ...
143 (x_i_x_H(10)*(1-dEps_dalpha_M_m_o))]; % d eps/ d alpha m = 0 for every iteration
144
145 Del_x_AC_b = 0; % init
146 for i=1:10 % Number of Fuselage Sections
147 Del_x_AC_b = Del_x_AC_b - (1/(q*C_L_alpha_w*S_w*mac_w))*(w_i(i)^2)*dEps_dalpha_i(i)*Del_x_i(i));
148 % Change in AC due to body
149 end
150
151 % Horizontal Tail Lift Slope Coefficient
152 k_H = 1+((8.2-(2.3*Lambda_LE_H))-AR_H*(0.22-(0.153*Lambda_LE_H)))/100;
% From Polhamus Formula
153 C_L_alpha_H = (2*pi*AR_H)/(2+sqrt(((AR_H^2*(1-M^2)/k^2)*(1+(((tan(Lambda_LE_half_H))^2)/(1-M^2))))+4));
% From Polhamus Formula
154
155 % Modelling of X_AC_wb
156 X_AC_wb = x_AC_w + Del_x_AC_b;
157
158 eta_H = 0.9; % Assumption
159 tau_e = 0.4; % Assumption
160
161 % Longitudinal Stability And Control Derivatives
162 C_L_alpha = C_L_alpha_w + (C_L_alpha_H*eta_H*(S_H/S_w)*dEps_dalpha);
163 C_L_delev = eta_H*(S_H/S_w)*C_L_alpha_H*tau_e;
164 C_L_i_H = eta_H*(S_H/S_w)*C_L_alpha_H;
165 C_m_alpha = (C_L_alpha_w*(X_cg - X_AC_wb)) - (C_L_alpha_H*eta_H*(S_H/S_w)* ...
166 (1-dEps_dalpha)*((X_AC_H - X_cg)/(mac_w)));
167 C_m_delev = -1*C_L_alpha_H*eta_H*(S_H/S_w)*tau_e*((X_AC_H - X_cg)/(mac_w));
168 C_m_i_H = -1*C_L_alpha_H*eta_H*(S_H/S_w)*((X_AC_H - X_cg)/(mac_w));
169
170 % C_L_alpha_dot and C_m_alpha_dot
171 C_L_alpha_dot = 2*C_L_alpha_H*eta_H*(S_H/S_w)*dEps_dalpha*((X_AC_H - X_cg)/(mac_w));
172 C_m_alpha_dot = -2*C_L_alpha_H*eta_H*((X_AC_H - X_cg)/(mac_w))^2*dEps_dalpha;
173
174 % Aircraft Aerodynamic Center
175 x_AC = (X_AC_wb + (C_L_alpha_H/C_L_alpha_w)*eta_H*(S_H/S_w)*(1-dEps_dalpha)* ...
176 X_AC_H/(mac_w))/(1 + (C_L_alpha_H/C_L_alpha_w)*eta_H*(S_H/S_w)*(1-dEps_dalpha));
177
178 % Static Margin
179 SM = (X_cg - x_AC)/(mac_w);
180
181 % Modelling C_L_q
182 B = sqrt(1 - ((M^2)*(cos(Lambda_LE_quarter)^2)));
183 C_L_q_w_o = (0.5 + 2*((x_AC_w - X_cg)/(mac_w)))*C_L_alpha_w_o;
184 C_L_q_w = ((AR + (2*cos(Lambda_LE_quarter)))/((AR*B) + (2*cos(Lambda_LE_quarter))))*C_L_q_w_o;
185 C_L_q_H = 2*C_L_alpha_H*eta_H*(S_H/S_w)*((X_AC_H - X_cg)/(mac_w));
186 C_L_q = C_L_q_H + C_L_q_w;
187
```

```

188 %% Modelling C_m_q
189 K_q = 0.7; % Correlation Coefficient from plot
190 C = (((AR*0.5*abs((x_AC_w - X_cg)/mac_w)) + (2*(abs((x_AC_w - X_cg)/mac_w)^2)))/ ...
191 (AR + (2*cos(Lambda_LE_quarter)))) + (((1/24)*(AR^3)*tan(Lambda_LE_quarter))/ ...
192 (AR + (6*cos(Lambda_LE_quarter)))) + (1/8);
193 C_m_q_w_o = -1*K_q*C_L_alpha_w_o*cos(Lambda_LE_quarter)*C;
194 C_m_q_w = (((((AR^3)*tan(Lambda_LE_quarter))/((AR*B) + (6*cos(Lambda_LE_quarter)))) + ...
195 (3/B))/((((AR^3)*tan(Lambda_LE_quarter))/((AR) + (6*cos(Lambda_LE_quarter)))) + (3)))*C_m_q_w_o;
196 C_m_q_H = -2*C_L_alpha_H*eta_H*(S_H/S_w)*(((X_AC_H - X_cg)/mac_w)^2);
197 C_m_q = C_m_q_w + C_m_q_H;
198
199 %% Vertical Tail Geometric Properties
200 b_2v = b_V*2;
201 % sq. ft - twice the span of vertical tail
202 lambda_V = C_t_V/C_r_V;
203 % Taper Ratio of the vertical tail
204 S_2v = 0.5*b_2v*C_r_V*(1+lambda_V);
205 % sq. ft - Area of the Vertical Tail
206 AR_V = (b_2v^2)/S_2v;
207 % Aspect Ratio Vertical Tail
208 mac_V = (2/3)*C_r_V*((1+lambda_V+lambda_V^2)/(1+lambda_V));
209 % ft - MAC of the Vertical Tail
210 Lambda_LE_V = Lambda_LE_V*pi/180; % rad
211 X_mac_V = ((b*(1+(2*lambda_V)))/(6*(1+lambda_V)))*tan(Lambda_LE_V);
212 % ft - Distance between LE of C_r_V and LE of mac_V
213 Y_mac_V = ((b*(1+(2*lambda_V)))/(6*(1+lambda_V)));
214 % ft - Distance between C_r_V and mac_V along Y
215 Lambda_LE_half_V = atan((tan(Lambda_LE_V))-((2*(1-lambda_V))/(AR_V*(1+lambda_V))));
216 % rad - Geometric Relation
217
218 %% Wing Horizontal Tail Geometric Properties
219 X_cg_r = X_mac_w + (X_cg*mac_w); % ft - Distance between LE of wing root and cg
220 X_V_s = X_WV_r + (mac_w/4) + X_mac_V - X_cg_r; % ft - Distance between cg and AC of mac_V
221 Z_V_s = y_V + Y_mac_V; % ft - Distance between FRL and mac_V
222 X_R_s = X_WV_r + X_AC_R - X_cg_r; % ft - Distance between cg and Rudder AC
223
224 %% Vertical Tail Lift Slope Coefficient
225 p_1 = b_V/(2*r1); % parameter for AR_V_eff
226 p_2 = Z_H/b_V; % parameter for AR_V_eff
227 p_3 = S_H/S_2v; % parameter for AR_V_eff
228 X_AC_H_V = X_mac_H + 0.25*mac_H; % parameter for AR_V_eff
229 p_4 = X_AC_H_V/mac_V; % parameter for AR_V_eff
230 c1 = 1.6; % from plot
231 c2 = 0.82; % from plot
232 K_HV = 1.05; % from plot
233 AR_V_eff = c1*AR_V*(1+(K_HV*(c2 - 1))); % Effect AR at Vertical Tail
234 k_V = 1+((8.2-(2.3*Lambda_LE_V))-AR_V_eff* ... % From Polhamus Formula
235 (0.22-(0.153*Lambda_LE_V))/100); % From Polhamus Formula
236 C_L_alpha_V_eff = (2*pi*AR_V_eff)/(2+sqrt(((AR_V_eff^2*(1-M^2)/k_V^2)* ...
237 (1+((tan(Lambda_LE_half_V))^2)/(1-M^2))))+4)); % 1/rad - From Polhamus Formula
238 C_L_alpha_V_eff_o= (2*pi*AR_V_eff)/(2+sqrt(((AR_V_eff^2*(1/k_V^2)* ...
239 (1+((tan(Lambda_LE_half_V))^2)/(1))))+4)); % 1/rad - From Polhamus Formula Mach = 0
240
241 %% Wing Body Contribution
242
243 %% Wing Contribution to the Dihedral Effect to the Geometric Dihedral Angle
244 C_L_beta_gamma_w = -1.6*(10^-4); % From Plot
245 par1 = AR/cos(Lambda_LE_half); % Parameter for K_m_gamma
246 par2 = M*cos(Lambda_LE_half); % Parameter for K_m_gamma
247 K_m_gamma = 1.08; % From Plot
248 C_L_beta_wb_gda = 57.3*gamma_W*(C_L_beta_gamma_w*K_m_gamma); % Dihedral Effect due to geometric dihedral angle
249
250 %% Wing contribution to the dihedral effect due to wing-fuselage position
251 d_B = sqrt(S_f_avg/0.7854); % ft - Fuselage Average Diameter

```

```

253 C_L_beta_wb_low_wing = (1.2*sqrt(AR)*Z_W*2*d_B)/(b^2);
254 % Dihedral Effect due to wing-fuselage position
255
256 %% Wing contribution to the Dihedral effect due to the Wing Sweep Angle
257 C_L_1 = W/(q*S_w); % C_L for the Flight Conditions
258 C_L1_C_L_beta = -0.5*(10^-3); % From plot
259 p1 = AR/(cos(Lambda_LE_half)); % Parameter for K_M_Lambda
260 p2 = M*cos(Lambda_LE_half); % Parameter for K_M_Lambda
261 K_M_Lambda = 1.05; % From Plot
262 p = A/b; % Parameter for K_f
263 K_f = 0.9; % From Plot
264 C_L_beta_wb_Lambda_w = 57.3*C_L_1*(C_L1_C_L_beta*K_M_Lambda*K_f);
265 % Dihedral effect due to the Wing Sweep Angle
266
267 %% Wing contribution to the Dihedral effect due to the Wing AR
268 C_L_beta_C_L1 = -1*(10^-3); % From Plot using lambda and AR
269 C_L_beta_wb_AR_w = 57.3*C_L_1*C_L_beta_C_L1; % Dihedral effect due to the Wing AR
270
271 %% Wing contribution to the dihedral effect due to wing twist angle
272 Del_C_L_beta_eps_tan_Del_c_4 = -2.25*(10^-5); % From Plot using AR and lambda
273 C_L_beta_wb_twist = 57.3*epsilon_W*(pi/180)*tan(Lambda_LE_quarter)* ...
274 Del_C_L_beta_eps_tan_Del_c_4; % Dihedral effect due to the Wing Twist
275
276 %% Fuselage contribution to the dihedral effect
277 Del_C_L_beta_gamma_w = -0.0005*AR*(d_B/b)^2; % Contribution
278 C_L_beta_wb_f_gda = 57.3*gamma_W*(C_L_beta_gamma_w*Del_C_L_beta_gamma_w);
279 % Dihedral Effect due to geometric dihedral angle
280
281
282 %% FINAL C_L_beta_wb
283 C_L_beta_wb = C_L_beta_wb_gda + C_L_beta_wb_low_wing + C_L_beta_wb_Lambda_w + ...
284 C_L_beta_wb_AR_w + C_L_beta_wb_twist + C_L_beta_wb_f_gda;
285
286 %% Vertical Tail Contribution
287 eta_V = 0.9; % Vertical Tail Efficiency
288 p1 = b_V/(2*r1); % Parameter for K_Y_V
289 K_Y_V = 0.76; % K_Y_V
290 eta_V_d_sigma_d_beta = 0.724 + (3.06*((0.5*S_2v/S_w)/ ...
291 (1+cos(Lambda_LE_quarter)))) + (0.4*Z_W/d) + (0.009*AR); % another term
292 C_L_beta_V = -1*K_Y_V*abs(C_L_alpha_V_eff)*eta_V_d_sigma_d_beta* ...
293 ((0.5*S_2v/S_w)/(1+cos(Lambda_LE_quarter)))*(((Z_V_s*cos(alpha*pi/180)) ...
294 -(X_V_s*sin(alpha*pi/180))/b)); % Vertical Tail Contribution
295
296 %% FINAL C_L_beta
297 C_L_beta = C_L_beta_wb + C_L_beta_V; % 1/rad - C_L_beta
298
299 %% Modelling C_Y_beta
300 C_Y_beta_w = -0.0001*abs(gamma_W)*57.3; % Wing Contribution
301 p = Z_W/(d/2); % Parameter for K_int
302 K_int = 0; % Mid Wing so 0
303 C_Y_beta_B = -2*K_int*(S_p_v/S_w); % Body Contribution
304 C_Y_beta = 0;
305 % Horizontal Tail 0 due to negligible dihedral angle
306 C_Y_beta_V = -K_Y_V*abs(C_L_alpha_V_eff)*eta_V_d_sigma_d_beta*(S_2v/S_w); % Vertical Tail Contribution
307 C_Y_beta = C_Y_beta_w + C_Y_beta_B + C_Y_beta_V; % C_Y_beta
308
309 %% Modelling C_n_beta
310 C_n_beta_w = 0; % Wing Contribution
311 p1 = l_cg/l_b; % Parameter for K_N
312 p2 = (l_b^2)/S_B_s; % Parameter for K_N
313 p3 = sqrt(z_1/z_2); % Parameter for K_N
314 p4 = z_max/w_max; % Parameter for K_N
315 K_N = 0.0002; % From Plot
316 Re_fuselage = Vp1*l_b/mu;
317 % Reynolds Number of Fuselage

```

```

318 K_RE_i = 1.7; % From Plot
319 C_n_beta_B = -57.3*K_N*K_RE_i*(S_B_s/S_w)*(l_b/b);
320 % Fuselage/Body Contribution
321 C_n_beta_V = -C_Y_beta_V*((X_V_s*cos(alpha*pi/180)) + (Z_V_s*sin(alpha*pi/180))/b);
322 % Vertical Tail Contribution
323 C_n_beta = C_n_beta_B + C_n_beta_V; % C_n_beta
324
325 %% Modelling C_L_p
326 Beta = sqrt(1 - M^2); % Beta
327 k = C_L_alpha_w*Beta/(2*pi); % k
328 p1 = Beta*AR/k; % Parameter for RDP
329 Lambda_beta = atan(tan(Lambda_LE_quarter)/Beta)*180/pi; % deg - Parameter for RDP
330 RDP = -0.40; % RDP
331 C_L_p_wb = RDP*k/Beta; % Wing Body Contribution
332 k_H = (C_L_alpha_H*Beta)/(2*pi); % k_H
333 p2 = Beta*AR/k_H; % Parameter for RDP_H
334 Lambda_beta_H = atan(tan(Lambda_LE_quarter_H)/Beta)*180/pi; % deg - Parameter for RDP_H
335 RDP_H = -0.49; % RDP_H
336 C_L_p_H = (RDP_H*Beta/k_H)*0.5*(S_H/S_w)*(b_H/b)^2; % Horizontal Tail Contribution
337 C_L_p_V = 2*C_Y_beta_V*((Z_V_s/b)^2); % Vertical Tail Contribution
338 C_L_p = C_L_p_V + C_L_p_H + C_L_p_wb; % C_L_p
339
340 %% Modelling C_n_r
341 C_n_r_C_L_1 = -0.2; % From Graph
342 C_n_r_w = C_n_r_C_L_1*C_L_1^2; % Wing Contribution
343 C_n_r_V = 2*C_Y_beta_V*((X_V_s*cos(alpha*pi/180)) + (Z_V_s*sin(alpha*pi/180))/(b^2)); % Vertical Tail Contribution
344 C_n_r = C_n_r_V + C_n_r_w; % C_n_r

```